14. Yamasaki Y, Ueda N, Kishimoto M, et al. Assessment of early stage autonomic nerve dysfunction in diabetic subjects-application of power spectral analysis of heart rate variability. *Diabetes Res* 1991;17:73-80.
15. Yonekura Y, Ishii Y, Torizuka K, Kadota K, Kambara H, Kawai C. Quantitative assessment of myocardial blood flow by measurement of fractional myocardial uptake of ^{201}Tl. *Kaku Igaku* 1980;17:1211-1220.
16. Peters AM. A unified approach to quantification by kinetic analysis in nuclear medicine. *J Nucl Med* 1993;34:706-713.
17. Merlet P, Valette H, Dubois-Rande JL, et al. Prognostic value of cardiac metaiodobenzylguanidine imaging in patients with heart failure [see comments]. *J Nucl Med* 1992;33:471-477.
18. Allman KC, Stevens MJ, Wieland DM, et al. Noninvasive assessment of cardiac diabetic neuropathy by carbon-11-hydroxyephedrine and positron emission tomography. *J Am Coll Cardiol* 1993;22:1425-1432.
19. Brismar T, Sima AA, Greene DA. Reversible and irreversible nodal dysfunction in diabetic neuropathy. *Ann Neurol* 1987;21:504-507.
20. Ganguly PK, Beamish RE, Dhalla KS, Innes IR, Dhalla NS. Norepinephrine storage, distribution and release in diabetic cardiomyopathy. *Am J Physiol* 1987;252:E734-E739.
21. Yoran C, Higginson L, Romero MA, Covell JW, Ross J Jr. Reflex sympathetic augmentation of left ventricular inotropic state in the conscious dog. *Am J Physiol* 1981;241:H857-H863.
22. Thames MD, Klopfenstein HS, Abboud FM, Mark AL, Walker JL. Preferential distribution of inhibitory cardiac receptors with vagal afferents to the inferoposterior wall of the left ventricle activated during coronary occlusion in the dog. *Circ Res* 1978;43:512-519.
23. Kobayashi H, Terada S, Kanaya S, et al. Artifactual defect of inferior myocardium on ^{123}I-metaiodobenzylguanidine myocardial SPECT: characteristic findings and preventive method on phantom study. *Kaku Igaku* 1994;31:359-366.
24. Wakasugi S, Fischman AJ, Babich JW, et al. Metaiodobenzylguanidine: evaluation of its potential as a tracer for monitoring doxorubicin cardiomyopathy. *J Nucl Med* 1993;34:1283-1286.

Simultaneous Evaluation of Fatty Acid Metabolism and Myocardial Flow in an Explanted Heart

Margot Jonas, Wolfgang Brandau, Bernhard Vollet, Michael Weyand, Anke Fahrenkamp, Franz-Josef Gildehaus, Joachim Sciuk, Hans H. Scheld and Otmar Schober

Departments of Nuclear Medicine, Cardiothoracic Surgery and Pathology, Westfälische Wilhelms University of Münster, Münster, Germany

The biodistribution of the fatty acid analog [^{131}I]PHIPA 3–10, was compared to the flow tracer ^{99m}Tc-sestamibi by quantitative analysis in a dual-isotope study performed during a heart transplantation. **Methods:** Iodine-131-PHIPA 3–10 and ^{99m}Tc-sestamibi were injected simultaneously approximately 20 min prior to the start of surgical procedure. Scintigraphic images of the sliced explanted heart were compared to the preoperative in vivo scans using [^{123}I]PHIPA 3–10, ^{201}Tl and ^{99m}Tc-sestamibi. In 14 tissue samples of the explanted heart, the radioactive contents from [^{131}I]PHIPA 3–10 and ^{99m}Tc-sestamibi were calculated as %ID/g-values and correlated with the corresponding histology. **Results:** In the preoperative scans, a mismatch of fatty acid uptake and perfusion ([^{123}I]PHIPA 3–10 > flow) was observed which indicated residual viable myocardium, while a matched defect was associated with scar. In viable myocardium, there was a significantly higher accumulation of [^{131}I]PHIPA 3–10 compared to ^{99m}Tc-sestamibi (mean 5.9×10^{-3} versus 2.7×10^{-3} %ID/g), whereas in scars the uptake of both tracers was comparable (1.2×10^{-3} versus 1.4×10^{-3} %ID/g). **Conclusion:** Myocardial viability can be defined more accurately with radioiodinated PHIPA 3–10 than with ^{99m}Tc-sestamibi. The differences of biodistribution in viable myocardium and scars indicate that not only perfusion but also the metabolic state of the myocardium can be evaluated with radioiodinated PHIPA 3–10.

Key Words: myocardial viability; iodine-123 fatty acid; dual-isotope study; pathology; heart transplantation

J Nucl Med 1996; 37:1990–1994

The detection of residual viable myocardium is an important factor in deciding whether to perform percutaneous transluminal coronary angioplasty (PTCA) or coronary bypass graft surgery (CABG). In many experimental and clinical trials, the use of radioiodinated free fatty acids (FFA) for assessment of myocardial viability has been elucidated (*1–4*). For enhancement of myocardial retention, various FFA analogs have been developed to inhibit rapid fatty acid catabolism by beta-oxidation (*5*). Most experience has been obtained with p-^{123}I-phenylpentadecanoic acid (p-IPPA) and p-^{123}I-β-methyl-IPPA (BMIPP) recently available in Japan (*1,2*).

Phenylene-bridged long-chain fatty acid analogs offer an alternative approach to methyl-branching to delay myocardial clearance and were first described by Liefhold and Eisenhut in 1987 and 1988 (*6,7*). In contrast to many other fatty acid analogs, [^{123}I]-PHIPA 3–10 (13-(p-[^{123}I]iodophenyl]-3-(p-phenylene)-tridecanoic acid) (Fig. 1) has a prolonged biological half-life in human myocardium (>15 hr), indicating metabolic trapping and is therefore more suited for SPECT investigations than unmodified phenyl fatty acids (*8–10*).

The aim of this study was to simultaneously examine [^{131}I]PHIPA 3–10 biodistribution compared to perfusion in the human myocardium. Myocardial accumulation of [^{131}I]PHIPA 3–10 and ^{99m}Tc-sestamibi was thus quantified in a dual-isotope study performed during heart transplantation. Distribution patterns and scintigraphic images of the heart in vivo and ex vivo were correlated to histological examination of the explanted heart.

MATERIALS AND METHODS

Radiopharmaceuticals

Iodine-123 and [^{131}I]PHIPA 3–10 were labeled by a non-carrier-added Cu(I)-assisted, nonisotopic halogen exchange (*11*). Briefly, ^{123}I or ^{131}I-sodium iodide were evaporated to dryness followed by the addition of the bromo-precursor and 5 μl of a CuCl solution (1 mg/ml acetic acid). After heating for 10 min at 180°C, the residue was dissolved in 200 μl absolute ethanol and purified by means of HPLC. The eluate was evaporated to dryness, dissolved in 150 μl ethanol, added dropwise to 10 ml of a solution of 5% human serum albumin and then filtered (0.22 μm). Thallium-201 and ^{99m}Tc-sestamibi were both commercially obtained.

Received Dec. 12, 1995; revision accepted Apr. 4, 1996.

For correspondence or reprints contact: Margot Jonas, MD, Department of Nuclear Medicine, Westfälische Wilhelms-Universität Münster, Albert-Schweitzer-Strasse 33, D-48129 Münster, Germany.

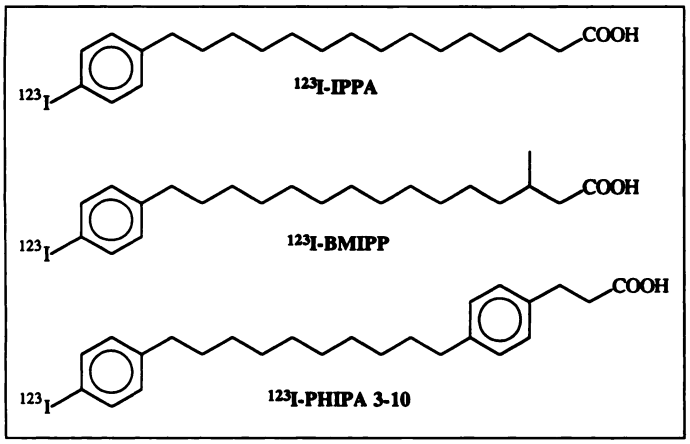

FIGURE 1. Chemical structures of IPPA, BMIPP and PHIPA 3–10.

Patients

All studies were subject to international law, approved by the local ethical committee and were performed after the patients gave written informed consent.

We studied a 49-yr-old man who had a posterolateral myocardial infarction 14 days earlier and consequently reduced left ventricular function. Coronary angiography revealed severe three-vessel disease. Contrast ventriculography (biplane) and echocardiography showed a dilated left ventricle with akinesia of the inferior wall, septum, apical and mid-anterior wall.

Within 4 wk, the patient underwent ^{201}Tl, ^{99m}Tc-sestamibi and [^{123}I]PHIPA 3–10 SPECT investigations prior to CABG. Six weeks after CABG and simultaneous implantation of a Novacor left ventricular assist device (*12*), a follow-up ^{99m}Tc-sestamibi control scan was acquired. During the following heart transplantation, a dual-isotope study using [^{131}I]PHIPA 3–10 and ^{99m}Tc-sestamibi was performed.

Heart In Vivo Scintigraphic Studies

After a light breakfast and subsequent fasting for 6–7 hr, the patient received 137 MBq of [^{123}I]PHIPA 3–10 under resting conditions. One and 3 hr p.i., SPECT was performed using a three-headed camera, ME collimators, 120 views, 3 × 40, 30 sec/view, 64 × 64 M, 360° NCO. Each view had 80,000–100,000 counts, and short-axis slices were reconstructed without prefiltering (Butterworth filter, 15th order, cutoff 0.55 Nyquist, without attenuation correction).

Flow studies were performed after injection of 750 MBq ^{99m}Tc-sestamibi (1.5 hr p.i.) or 100 MBq ^{201}Tl (4 hr p.i.) using a single-headed camera, LEAP collimator, 32 views, 180°, 64 × 64 M, (Butterworth filter, 5th order, cutoff 0.55 Nyquist, without attenuation correction, background subtraction 30%).

Thallium-201-scans were performed without anti-anginal drugs, ^{99m}Tc-sestamibi and [^{123}I]PHIPA studies (n = 3–10) were performed under the patient's usual medication.

Explanted Heart: Dual-Isotope Study

Iodine-131-PHIPA (53 MBq) and 900 MBq ^{99m}Tc-sestamibi were injected simultaneously approximately 20 min before surgery. Immediately before clamping the aorta (50 min p.i.), the blood concentration of both tracers was determined from a venous blood sample. The explanted heart was cut into 1-cm thick slices parallel to the atrioventricular sulcus and preserved in formaldehyde.

Planar images of the cardiac slices were acquired (1800 sec/energy window, ME collimator, 256 × 256 M). The energy discriminators were centered on 364 keV for ^{131}I and on 140 keV for ^{99m}Tc with 15% windows.

Tissue samples were taken from areas which, by visual inspection appeared to be viable (n = 11) or scared (n = 3) (see Fig. 3A).

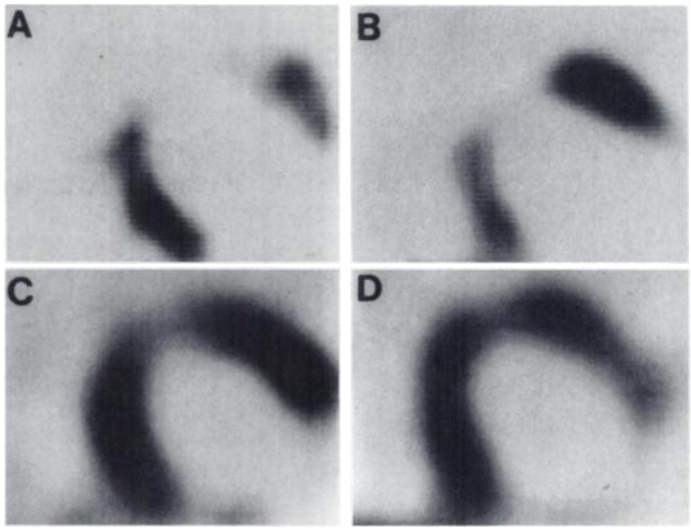

FIGURE 2. SPECT imaging of the heart in vivo (short axis-slices of the mid left ventricle). Perfusion defect in the anterior wall: (A) ^{201}Tl redistribution. (B) ^{99m}Tc-sestamibi. (C) Reduced but relevant [^{123}I]-PHIPA 3–10 uptake in the anterior wall indicating residual viable myocardium. (D) Improved perfusion with ^{99m}Tc-sestamibi in the anterior wall after CABG. (A–D) Matched defect posterolateral representing scar.

They were evaluated histologically and monitored for ^{99m}Tc and ^{131}I activities in an automatic well counter. After correction for physical decay and crossover of ^{131}I activity into the ^{99m}Tc window (6%), the count rates were calculated as %ID/g. Calibration was performed by measurement of diluted aliquots of the original solutions of [^{131}I]PHIPA 3–10 and ^{99m}Tc-sestamibi.

The differences in myocardial uptake between the [^{131}I]PHIPA 3–10 and ^{99m}Tc-sestamibi were statistically evaluated using the paired t-test. The significance of the differences in means between both groups were analyzed by Student's t-test.

RESULTS

In Vivo Scintigraphic Imaging

Because of a history of posterolateral infarction, the patient exhibited an extended defect in the posterolateral wall with ^{201}Tl and ^{99m}Tc-sestamibi as well with [^{123}I]PHIPA 3–10 (Fig. 2). In spite of akinesia detected by echocardiography and contrast ventriculography, the septum was visualized as viable with all three tracers according to the intraoperative macroscopic findings. The anterior wall revealed a defect in the ^{201}Tl and ^{99m}Tc-sestamibi scintigrams corresponding to akinesia and insufficiently collateralized LAD stenosis. In contrast, [^{123}I]PHIPA 3–10 showed a reduced but significant uptake in this lesion indicating residual viable myocardium. Viability could be confirmed in a follow-up study 6 wk after revascularization, in which the accumulation of ^{99m}Tc-sestamibi was significantly increased in the anterior wall.

Despite locally improved perfusion, the overall function of this terminally ill heart deteriorated during bypass surgery, thus heart transplantation became unavoidable. Between the time of scintigraphic follow-up after revascularization and heart transplantation 6 wk later, the patient showed no significant cardiac events.

Explanted Heart: Morphology

An extensive posterolateral scar, multiple areas of predominantly subendocardial, focal scarring and widespread endocardial fibrosis could be distinguished in the left ventricle of the explanted heart, even by gross inspection (Fig. 3A). From microscopic examination, the myocardium of the posterolateral wall was replaced nearly completely by fibrous tissue. The only

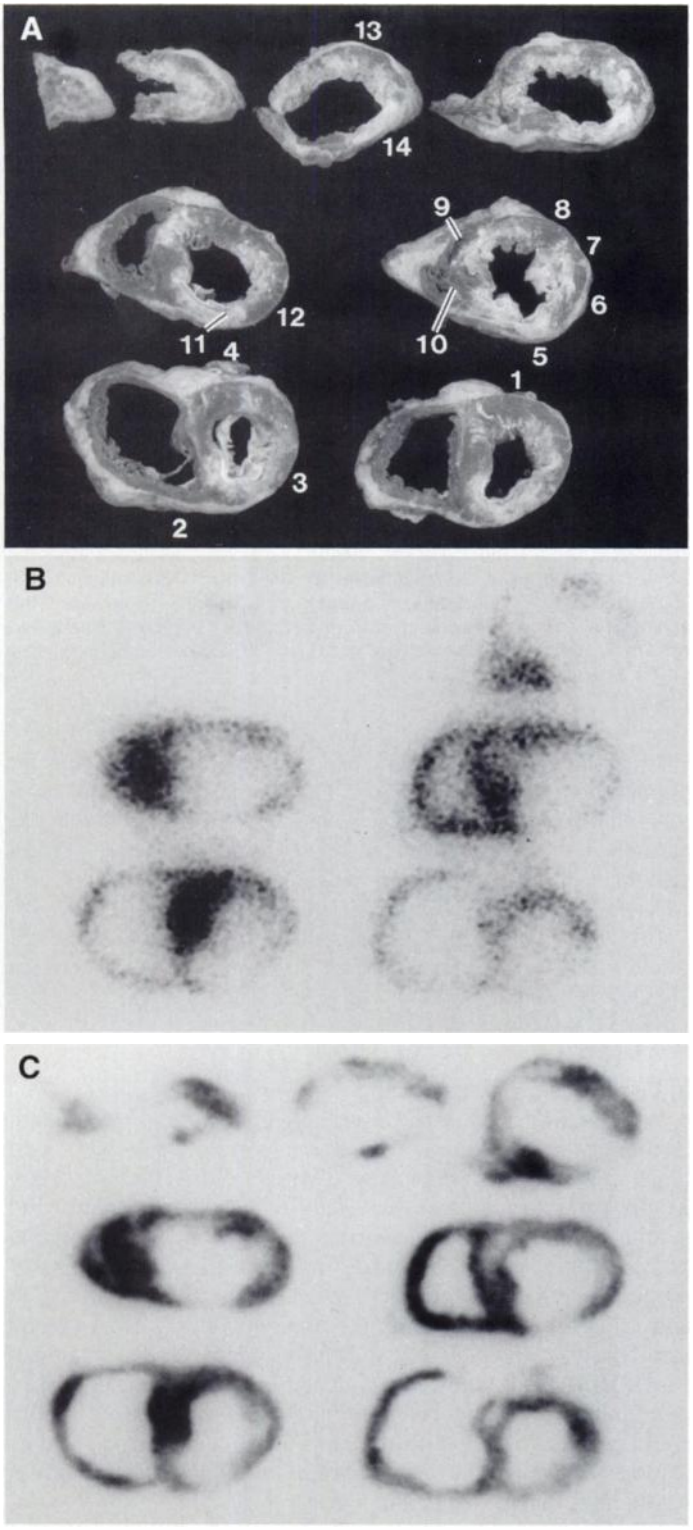

FIGURE 3. Explanted heart cut into 1-cm thick slices parallel to the atrioventricular sulcus. (A) Locations of tissue sampling. Macroscopic findings: transmural scar posterolateral, rest of myocardium predominantly viable with endocardial and patchy interstitial fibrosis. Dual-isotope scintigraphies with (B) [^{131}I]PHIPA 3–10 and (C) ^{99m}Tc-sestamibi.

few remaining myocytes exhibited severe myofibrillar lysis and enlarged nuclei. Intact myocardium predominated in the anterolateral, septal and anterior wall. Histologically, the subendocardial scarring was only minor in the anterior wall. No acute myocytolysis or recent myocardial infarction were delineated. The histological findings correspond to severe multivessel disease, including subtotal stenosis of the LAD and Cx. In contrast to coronary angiography with only 50% stenosis, a long obliteration of the RCA was detected in the pathological examination.

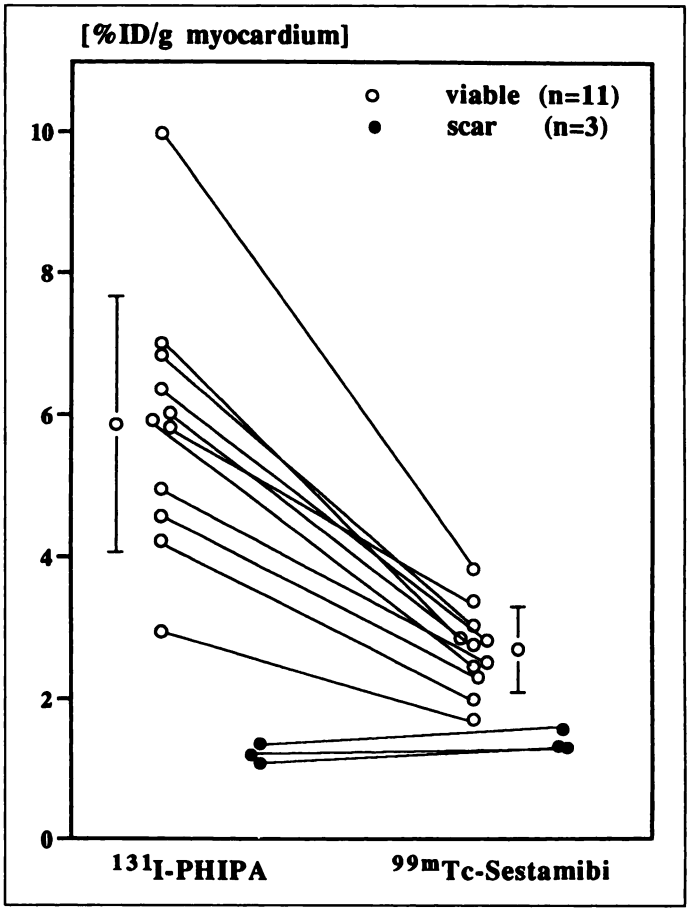

FIGURE 4. Absolute myocardial uptake of [^{131}I]PHIPA 3–10 and ^{99m}Tc-sestamibi in different tissue samples after explantation, mean and s.d.

Explanted Heart: Dual-Isotope Study

Scintigraphy. Technetium-99m-sestamibi and [^{131}I]PHIPA scintigrams of the sliced explanted heart matched the histological findings (Fig. 3B,C). Although the accumulation of both tracers might be globally reduced, the septal, anterolateral and anterior wall could be identified as viable myocardium. There was a large defect in the posterolateral wall observed with ^{99m}Tc-sestamibi as well with [^{131}I]PHIPA 3–10 especially in the mid-ventricle. Compared to the explanted heart, there was a similar distribution of [^{123}I]PHIPA 3–10 and ^{99m}Tc-sestamibi (after revascularization) in the heart in vivo (Fig. 2).

Biodistribution in Myocardial Tissue Samples. In the 14 tissue samples (Fig. 3A) of the explanted heart, the myocardial accumulation of [^{131}I]PHIPA 3–10 and ^{99m}Tc-sestamibi, calculated as %ID/g myocardium, was compared to the corresponding histology (Fig. 4). Eleven of these 14 samples were histologically proven as viable and three samples of the inferior wall as scars.

In viable myocardium, [^{131}I]PHIPA 3–10 uptake showed a widespread variation but was always higher than ^{99m}Tc-sestamibi uptake (Fig. 4). The differences between [^{131}I]PHIPA 3–10 and ^{99m}Tc-sestamibi uptake (mean ± s.d.: $5.9 \pm 1.8 \times 10^{-3}$ versus $2.7 \pm 0.6 \times 10^{-3}$ %ID/g) were statistically highly significant ($p < 0.0001$). Whereas the [^{131}I]PHIPA 3–10/^{99m}Tc-sestamibi uptake ratio was about 2:1 in viable myocardium, in scars, however, the accumulation of ^{99m}Tc-sestamibi was slightly, but significantly, higher than that of [^{131}I]PHIPA 3–10

(mean ± s.d.: 1.4 ± 0.1 × 10^{-3} versus 1.2 ± 0.1 × 10^{-3} %ID/g; $p < 0.0448$).

Venous blood sampling, prior to explantation, revealed that only minor amounts of the injected activities remained in the blood at 50 min p.i.: [^{131}I]PHIPA 3–10: approx. 15 %ID, ^{99m}Tc-sestamibi: approx. 3 %ID assuming a total blood volume of 5.5 liter).

DISCUSSION

In coronary artery disease, differences between regional radioiodinated fatty acid uptake and blood flow have frequently been reported in infarcted myocardium. Two general mismatch patterns, FFA > flow and FFA < flow, have been observed (*13–21*). The more frequent phenomenon (FFA < flow) corresponds to hibernating or stunned myocardium (*13*), which may point to a metabolic shift from FFA to glucose utilization (*14*). This mismatch was found to be far more prevalent in areas showing dyskinesia, acute infarction and/or reperfusion after thrombolysis or PTCA (*15–18*). Thus, it may indicate persistent metabolic abnormality associated with the failure of functional recovery after revascularization, particularly in the early phase of acute infarction (*1,17*). Excess of fatty acid uptake (FFA > flow) has been proven as a sensitive indicator for residual, viable myocardium (*16,19–21*). Enhanced [^{123}I]BMIPP uptake was often related to akinetic or dyskinetic areas subserved by occluded arteries or previous infarction without emergent reperfusion interventions. This mismatch pattern was interpreted as increased metabolic demands of passive systolic wall stretch (*1,17*).

In the present study, myocardial viability could be delineated by preserved [^{123}I]PHIPA 3–10 accumulation regardless of severely reduced flow. Regarding the patient's history (infarction without thrombolysis), coronary anatomy (insufficiently collateralized LAD-occlusion) and dysfunction proof (akinesia), these results are in agreement with the findings observed with BMIPP (*1,17*).

Following CABG the perfusion increased in the akinetic area with preserved [^{123}I]PHIPA 3–10 uptake (FFA > flow) indicating hibernating myocardium (Fig. 2). Furthermore, viability could be confirmed histologically. The question remains, however, whether this mismatch pattern may predict salvageable myocardium with functional recovery after revascularization. Despite improved regional perfusion, the overall cardiac function deteriorated during CABG, so that a heart transplantation became unavoidable. Due to the implantation of the Novacor left ventricular assist device, which prevented motion analysis, regional functional outcome could not be determined.

Areas with FFA > flow (anterior wall) revealed no morphological differences compared to areas with concordant, moderately reduced tracer uptake. Both phenomena represented predominantly viable tissue, while the whole myocardium revealed degenerative alterations due to chronic ischemia. The matched [^{123}I]PHIPA 3–10 and perfusion defect could be confirmed as transmural scar (Fig. 3).

Confirmation of viability by histological examination has been performed only in a limited number of studies (*22*). Additionally, transmural myocardial biopsy requires much caution to obtain representative tissue samples (*21,23,24*). Because quantitation of SPECT data is not possible so far, the current study provides the first quantitative results on the distribution of gamma emitting radiopharmaceuticals in human myocardium. Moreover, performing a dual-isotope study permitted that information on metabolism and myocardial perfusion could be obtained simultaneously.

Despite the close relation of myocardial fatty acid uptake with regional flow and the sensitivity of cardiac fatty acid oxidation to oxygen deprivation, viable myocardium always revealed a significantly higher PHIPA 3–10 than sestamibi accumulation (Fig. 4). In contrast, the distribution pattern changed in scars (PHIPA 3–10 ≤ flow). Although the analysis of scars was limited to only three regions, these differences are statistically significant as well. Interference of blood pool with myocardial activity could be excluded because of the very fast blood clearance of both tracers ($t_{1/2PHIPA}$ = 7 min) (*8,9*).

As both tracers are trapped in the myocardium without significant washout (*8,9*), different distribution patterns reflect characteristic physiological differences of both tracers revealing myocardial extraction of radioiodinated PHIPA 3–10 is more dependent on myocardial viability than the uptake of ^{99m}Tc-sestamibi. The pronounced differences between [^{123}I]PHIPA 3–10 and ^{99m}Tc-sestamibi implicate a more accurate scintigraphic differentiation of viable from scared myocardial tissue and support the hypothesis that [^{123}I]PHIPA 3–10 might serve as metabolic marker for myocardial SPECT investigations. The biochemical mechanisms affecting flow independent PHIPA 3–10 extraction, resulting in such distribution patterns are not well understood so far and require further evaluation.

CONCLUSION

Iodine-123-PHIPA 3–10 is a promising fatty acid analog, which is metabolically trapped in the myocardium with a long biological half life of more than 15 hr, permitting SPECT imaging. Our results imply that residual viable myocardium can be differentiated more accurately from scars with radioiodinated PHIPA 3–10 than with ^{99m}Tc-sestamibi. Furthermore, the different biodistribution of [^{131}I]PHIPA 3–10 and ^{99m}Tc-sestamibi in chronic ischemic myocardium and scars indicates that not only the perfusion, but the metabolic state of the myocardium can be evaluated with radioiodinated PHIPA 3–10. As a metabolic marker of the heart [^{123}I]PHIPA 3–10 has the potential to improve the assessment of myocardial viability with SPECT.

REFERENCES

1. Knapp FF Jr, Franken P, Kropp J. Cardiac SPECT with iodine-123-labeled fatty acids: evaluation of myocardial viability with BMIPP. *J Nucl Med* 1995;36:1022–1030.
2. Reske SN. Viability as seen with radiolabeled fatty acids—a new approach to a challenging problem. *Eur J Nucl Med* 1994;21:279–282.
3. Hansen CL. Preliminary report of an ongoing phase I/II dose range, safety and efficacy study of iodine-123-phenyl-pentadecanoic acid for the identification of viable myocardium. *J Nucl Med* 1994;35(suppl):38S–42S.
4. Kropp J, Fehske W, Krois M, et al. Influence of revascularization on myocardial perfusion, metabolism and function. *Ann Nucl Med* 1993;7:69–78.
5. Knapp FF Jr, Kropp J. Iodine-123-labeled fatty acids for myocardial single-photon emission tomography: current status and future perspectives. *Eur J Nucl Med* 1995;22:361–381.
6. Liefhold J. Phenylenverbrückte radiojodmarkierte Phenylfettsäuren (PHIPA). PhD thesis. University of Heidelberg, 1987.
7. Eisenhut M, Liefhold J. Radioiodinated p-phenylene bridged fatty acids as new myocardial imaging agents: syntheses and biodistribution in rats. *Appl Radiat Isot* 1988;39:639–649.
8. Brandau W, Gildehaus F-J, Puskás C, et al. Iodine-123-iodo-PHIPA 3–10: a metabolic marker for myocardial SPECT investigations [Abstract]. *Eur J Nucl Med* 1994;21:786.
9. Jonas M, Brandau W, Vollet B, et al. Iodine-123-PHIPA 3–10: a SPECT tracer for assessment myocardial viability [Abstract]. *Eur J Nucl Med* 1994;21:736.
10. Zehelein J, Bubeck B, Eisenhut M, Hoffend J, Zimmermann R. Iodine-123 PHIPA scintigraphy in chronic coronary artery disease: a comparative study with ^{201}Tl [Abstract]. *J Nucl Cardiol* 1995;2(suppl):S98.
11. Coenen HH, Dutschka KP, Brandau W. N.c.a. Cu(I)-assisted iodine-exchange on N-alkylated ortho-, meta- and para bromobenzamides. *J Lab Compd Radiopharm* 1994;35:222–223.
12. Charron M, Follansbee W, Ziady GM, Kormos RL. Assessment of biventricular cardiac function in patients with a novacor left ventricular assist device. *J Heart Lung Transplant* 1994;13:263–267.
13. Franken PR, De Geeter F, Dendale P, et al. Abnormal free fatty acid uptake in subacute myocardial infarction after coronary thrombolysis: correlation with wall motion and inotropic reserve. *J Nucl Med* 1994;35:1758–1765.
14. Tamaki N, Tadamura E, Kudoh T, et al. Prognostic value of iodine-123-labeled BMIPP fatty acid analog imaging in patients with myocardial infarction. *Eur J Nucl Med* 1996;23:272–279.

15. Tamaki N, Kawamoto M, Yonekura Y, et al. Regional metabolic abnormality in relation to perfusion and wall motion in patients with myocardial infarction: assessment with emission tomography using an iodinated branched fatty acid analog. *J Nucl Med* 1992;33:659–667.
16. Saito T, Yasuda T, Gold HK, et al. Differentiation of regional perfusion and fatty acid uptake in zones of myocardial injury. *Nucl Med Commun* 1991;12:663–675.
17. De Geeter F, Franken PR, Knapp FF Jr, Bossuyt A. Relationship between blood flow and fatty acid metabolism in subacute myocardial infarction: a study by means of ^{99m}Tc-sestamibi and ^{123}I-β-methyl-iodo-phenyl pentadecanoic acid. *Eur J Nucl Med* 1994;21:283–291.
18. Nishimura T, Uehara T, Shimonagata T, Nagata S, Haze K. Clinical experience of ^{123}I-BMIPP myocardial imaging for myocardial infarction and hypertrophic cardiomyopathy. *Ann Nucl Med* 1993;7:35–40.
19. Henrich MM, Visser E, von der Lohe E, et al. The comparison of 2-^{18}F-2-deoxyglucose and 15-(ortho-^{123}I-phenyl)-pentadecanoic acid uptake in persisting defects on thallium-201 tomography in myocardial infarction. *J Nucl Med* 1991;32:1353–1357.
20. Kuikka JT, Mussalo H, Hietakorpi S, Vanninen E, Länsimies E. Evaluation of myocardial viability with technetium-99m hexakis-2-methoxyisobutyl isonitrile and iodine-123 phenyl-pentadecanoic acid and single photon emission tomography. *Eur J Nucl Med* 1992;19:882–889.
21. Murray GL, Schad NC, Magil HL, Vander Zwagg R. Myocardial viability assessment with dynamic low-dose iodine-123-iodophenylpentadecanoic acid metabolic imaging: comparison with myocardial biopsy and reinjection SPECT thallium after myocardial infarction. *J Nucl Med* 1994;53(suppl):43S–48S.
22. Delbeke D, Lorenz CH, Votaw JR, et al. Estimation of left ventricular mass and infarct size from nitrogen-13-ammonia PET images based on pathological examination of explanted human hearts. *J Nucl Med* 1993;34:826–833.
23. Murray G, Schad N, Ladd W, et al. Metabolic cardiac imaging in severe coronary disease: assessment of viability with iodine-123-iodophenylpentadecanoic acid and multicrystal gamma camera and correlation with biopsy. *J Nucl Med* 1992;33:1269–1277.
24. Vanoverschelde J-L, Wijns W, Depré C, et al. Mechanism of chronic regional postischemic dysfunction in humans: new insights from the study of noninfarcted collateral-dependent myocardium. *Circulation* 1993;87:1513–1523.

(continued from page 7A)

FIRST IMPRESSIONS

What Is the Radiopharmaceutical? What Are the Findings?

Figure 1.

PURPOSE

This case does not depict a liver scan with a lot of free pertechnetate in the sulfur colloid preparation, but rather a 21-yr-old woman with adenocarcinoma of the pelvis. Her pathologic specimen demonstrated features of neuroendocrine tumor which resulted in a referral for a ^{111}In-pentetreotide scan to evaluate extent of disease. The 4-hr whole-body image (Fig. 1) showed multiple foci of intense radiotracer uptake in the pelvis and lower abdomen, which confirmed the tumor masses seen on MRI and confirms the somatostatin receptor positive status. Normal uptake was seen in the liver, spleen and thyroid.

The interesting feature in the image is the large stomach-shaped uptake in the upper abdomen, which is suspicious for a large tumor. Note, however, the absence of renal activity, which is usually seen in this type of study. The patient had crossed-fused ectopia of the left kidney, which was positioned anterior to the lower lumbar spine and was fused to the lower pole of the right kidney, resulting in the stomach-shaped finding that could have been mistaken for a somatostatin receptor-positive tumor.

This case illustrates the importance of knowing the normal distribution of a radiopharmaceutical to properly interpret images. The availability and awareness of findings on correlative imaging findings is also useful.

TRACER

Indium-111-pentetreotide, 6 mCi

ROUTE OF ADMINISTRATION

Intravenous

TIME AFTER INJECTION

Four hours

INSTRUMENTATION

ADAC Dual Genesys gamma camera with medium-energy, general-purpose collimator

CONTRIBUTORS

Henry Yeung and Homer Macapinlac, Memorial Sloan-Kettering Cancer Center, New York, New York